Journal of Computer and Communications, 2025, 13(10), 23-48
https://www.scirp.org/journal/jcc
ISSN Online: 2327-5227
ISSN Print: 2327-5219

An Efficient Placement Approach of Visual Sensors under Observation Redundancy and Communication Connectivity Constraints

Yves Faga, Frantz Tossa, Wahabou Abdou, Julien Dubois

ImViA Laboratory, EA 7535, University of Burgundy, Dijon, France
Email: yvespohowe@gmail.com

How to cite this paper: Faga, Y., Tossa, F., Abdou, W. and Dubois, J. (2025) An Efficient Placement Approach of Visual Sensors under Observation Redundancy and Communication Connectivity Constraints. *Journal of Computer and Communications*, **13**, 23-48.
https://doi.org/10.4236/jcc.2025.1310002

Received: August 8, 2025
Accepted: October 7, 2025
Published: October 10, 2025

Abstract

Visual Sensor Networks (VSNs) focus on capturing data, extracting relevant information, and enabling communication. However, the presence of obstacles affects network efficiency, linking data quality to camera positioning. Deploying multiple cameras strategically in complex areas while maintaining node communication is a key challenge. This paper proposes a method for optimizing VSN deployment in 2D indoor environments. The approach integrates multi-objective optimization criteria: maximizing overall coverage, observing zones of interest, ensuring redundancy, and maintaining communication connectivity. The method simulates environments with cameras, obstacles, and zones of interest, evaluating camera placement based on defined objectives. By optimizing camera positions and orientations, the method achieves up to 100% coverage, even in areas with obstacles. Compared to existing approaches, this method consistently ensures high coverage and communication connectivity, making it more effective in challenging indoor environments.

Keywords

Visual Sensor Networks (VSNs), Deployment Optimization, Overall Coverage, Zones of Interest Observation, Connectivity

1. Introduction

Sensor networks have been a subject of research for several decades. When these networks incorporate cameras, they are referred to as Visual Sensor Networks (VSNs). A VSN regroups small visual sensor nodes, each one including an image sensor and a communication module [1]. Data analysis can be centralized, requiring the transfer of data to a central processing unit, or distributed across the network. VSNs offer innovative solutions for various applications, providing information-rich descriptions of captured events. They find natural applications in video surveillance, facilitating the detection and tracking of people [2] [3], as well as in diverse fields such as agriculture [4] and the military [5]. To address the deployment's quality, it is imperative to evaluate predefined metrics aligned with the application's objectives. In network deployment studies, the typical objective is coverage, encompassing the overall study field, the presence of zones of interest in the scene (ZoI), etc. Some applications consider ZoI as a grouping of a set of target points. When targets are present in the scene, each target may require observation by multiple cameras to mitigate information loss. The incorporation of redundant observations of targets could be crucial to mitigate particular acquisition uncertainties or, alternatively, to offer a multi-view perspective of the area. Once the targets are observed, sensor nodes can communicate with each other and transmit the acquired data. This emphasizes that the positioning of cameras is crucial for acquiring relevant information for potential data analysis. Deploying visual sensors in a potentially obstructed scene must simultaneously adhere to the aforementioned application objectives, and is not trivial.

This paper deals with a multi-objective optimization problem of a VSN in a 2-dimensional (2D) indoor environment considering obstacles and integrating the notions of redundant coverage and communication. It is an extension of a preliminary work [6] which includes observation redundancy, communication requirements and new experiments. We propose an optimization approach which combines two interconnected modules: a visual coverage simulator based on the ray-tracing method, and an optimization module using a genetic algorithm. For an effective deployment of a VSN, the different camera parameters (orientation angle, opening angle, position of the camera in the plane) must be adjusted. The position and the orientation of the cameras are gradually refined through an optimization process to meet the application requirements while taking into account the characteristics of the study zone. This deployment must allow us to acquire data from the scene and to evaluate them while respecting the configuration of the complex scene. The paper is organized as follows. Section 2 features some related work. The problem of deploying visual sensor nodes is formalized in Section 3. Then, Section 4 describes the proposed optimization platform and its main modules. Experiments and results are presented and discussed in Section 5. Finally, Section 6 presents the paper's contributions and proposes future works.

2. Related Works

The efficiency of data collection in sensor networks is largely influenced by the positioning of the sensors within the study zone. Various sensor placement methods are found in the literature [7] [8], generally classified into two main categories: random and deterministic. Random deployment is typically used for large, unknown study zones [9], while deterministic deployment ensures a homogeneous placement through a grid layout of sensors, allowing full supervision of the area [10]. One of the most studied types of sensors in the literature is visual sensors

[11] [12], due to their ability to capture rich information from observed scenes [13]. The placement of visual sensors, such as cameras [7], must ensure effective monitoring of the study area, meeting specific objectives depending on the application. It is essential to consider scene parameters, such as obstacles or areas of interest, which influence network efficiency. Obstacles within the study zone generally pose challenges, reducing network performance in both data acquisition and transmission [14]. Given the complexity of these scenes, efficient automatic camera deployments can be carried out based on state-of-the-art criteria.

Coverage is one of the most critical criteria in the literature [15]. Three main types of coverage are typically considered [16]: zone coverage, which aims to maximize coverage of the entire area [17]; region or target coverage, focusing on covering specific targets within the study zone [18]; and barrier coverage, which is used for intrusion detection along a barrier [19]. In this study, we focus on optimizing the placement of cameras in a 2D environment with potential obstacles to maximize the coverage of the observed area [6] [18]. Some works in the literature propose random camera placement with fixed viewing angles in a 2D environment [20] [21], which simplifies environment representation and reduces simulation computation time. While the 2D model is widely used [22]-[27], other studies also explore 3D coverage optimization [28]-[31]. In both cases, the positioning and orientation of cameras are adjusted to optimize coverage. However, this approach only allows visualization of the camera's field of view, necessitating more efficient placement solutions that account for factors such as position, orientation angle, aperture, and range.

In certain applications, targets need to be covered by multiple sensors, a concept known as K-coverage [32]. Redundant coverage not only enhances the total coverage but also increases the robustness of the network, improving fault tolerance in the event of sensor failure. In K-coverage, a point is considered redundant if it is observed by at least two cameras ($K \geq 2$) [32]. Redundancy optimization is crucial depending on the specific requirements of an application. Some applications aim to maximize redundancy [33], while others seek to minimize it to save resources. For instance, redundant nodes can serve as backups in case of failures [34], or be put on standby to prolong the network's operational life. Alaei *et al.* [35] suggest a threshold for redundancy coverage, beyond which redundant sensors are put on standby. Other works focus on maximizing redundancy to ensure high data quality [36]. The concept of K-coverage is often used to guarantee the quality of target acquisition [37] [38], ensuring that multiple perspectives cover important points of interest. Some studies propose random sensor deployments in obstacle-free zones to maximize redundancy through the collection of data from various perspectives [39] [40]. Costa *et al.* [41] address the target coverage problem by incorporating redundancy as an objective parameter in an evolutionary algorithm to ensure that all targets are covered. In addition to coverage, connectivity is a crucial constraint in Visual Sensor Networks (VSNs). A network is considered fully connected if a path exists between every pair of nodes, enabling data exchange across the network. Connectivity is a key objective in many VSN applications [42], with some studies aiming to optimize it [43]. However, full connectivity is not always required, and in some cases, the network can function with several connected components.

To achieve effective camera placement for good coverage and redundancy, automatic methods are typically based on optimization techniques. These methods can be categorized into two groups: exact methods, such as Integer Linear Programming and Monte Carlo simulations, which evaluate all possible solutions to find the optimal one [44]; and approximate methods, such as evolutionary algorithms, simulated annealing, Taboo search, and gradient descent, which provide a near-optimal solution within a reasonable time frame [45]. Approximate methods may rely on either a single solution that is iteratively improved [46], or a population of solutions whose overall quality is enhanced over successive iterations [47]. In [41], the authors propose a Centralized Prioritized Greedy Algorithm (CPGA) to automatically determine the orientations of visual sensors, thereby improving redundant coverage of known targets. This algorithm focuses on prioritizing relevant targets, identified as critical in video surveillance contexts. Similarly, Silva *et al.* [48] present two methods: ECPGA (Enhanced Centralized Prioritized Greedy Algorithm), an extension of CPGA that increases the range of camera orientations, and RCMA (Redundancy Coverage Maximization Algorithm), which optimizes total coverage and redundancy simultaneously. These methods are designed to maximize coverage while ensuring redundancy in critical areas.

Rangel *et al.* [18] and Silva *et al.* [48] address the issue of optimizing redundant coverage by proposing algorithms that adjust the orientation of cameras to cover as many targets as possible. The objectives of these studies focus on maximizing coverage and optimizing redundancy. Rangel *et al.* present two multi-objective optimization methods: the lexicographic method, where priority is established before the optimization process begins, and the hindsight method, which assesses priority at the end of the optimization. Their comparative study shows that the hindsight method provides better results but comes at a higher computational cost. In conclusion, this study focuses on efficiently positioning cameras in an indoor environment with potential obstacles and areas of interest. The optimization criteria include region coverage, target coverage, and considerations of redundancy and connectivity. Evolutionary optimization methods offer effective solutions for balancing these criteria and enhancing the overall performance of visual sensor networks.

3. Sensor Modeling and Deployment Assessment Metrics

This section describes the visual sensor model used, as well as the metrics used to evaluate the quality of a VSN deployment.

3.1. Sensor Modeling and Observation Process

We consider visual sensor nodes provided with directional cameras. Each camera has a restricted Field of View (FoV), defining the area where objects can be detected. The FoV size depends on the camera's viewing angle and range (viewing distance). This paper examines the placement of a VSN in a two-dimensional plane, meaning all cameras are positioned at the same altitude. Sensors can only be adjusted horizontally, with no tilt or zoom capabilities. As illustrated in **Figure 1**, each camera is defined by its Cartesian coordinates (x, y), its field of view angle α , its orientation angle θ, and its viewing range R . The parameters α and R are considered intrinsic physical characteristics of the cameras and are treated as fixed inputs. Therefore, the optimization problem consists of determining the efficient coordinates (x, y) and orientation angle (θ) for each camera.

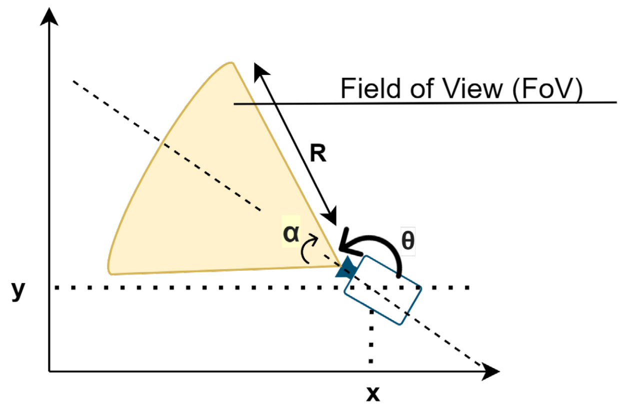

Figure 1. Camera's parameter.

To evaluate the coverage, we use the ray-tracing method, which is one of the most efficient in terms of realism [49] and allows to accurately compute the coverage area [6]. Its principle is to generate an image in which each pixel is independently processed [50]. A ray is launched from the camera towards the plane, and at each intersection, the nature and position of the corresponding pixel is determined [51]. This technique is used to determine whether a pixel is observed. The concepts of reflections and refractions are not addressed in this work.

3.2. Visual Observation Metrics

Four metrics related to visual observation are considered to evaluate the quality of a VSN deployment.

- *The overall coverage area*

This metric is the ratio of the area observed by the cameras to the total area of the study field. To compute this criterion we consider the cumulative FoV of the different cameras. Note that the presence of obstacles in the study field can obstruct target in the study zone.

- *The target coverage*

A target is considered observed if at least one camera can detect it. First, the FoV of each camera is determined on the basis of the ray-tracing method. Then, given the target position, the Euclidean distance between the target and all cameras is estimated. Finally, we test whether the target's position is included in the field of view of all potential cameras close enough to it. In this way, we can simulate scenarios such as buildings with obstacles that make the study zone more complex; and also define Zone of Interest (ZoI) formed by several target points. Figure 2 illustrates an example of a study zone with obstacles (wall partitions) and ZoI. We have defined a minimum of ρ target points coverage for a ZoI to be considered as covered. In the current study $\rho = 80\%$.

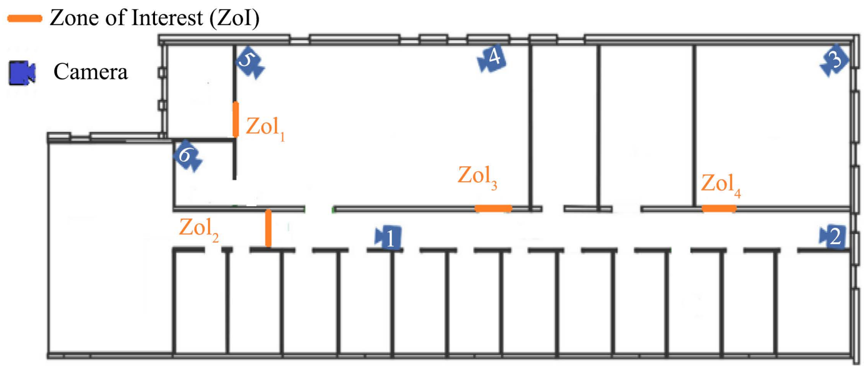

Figure 2. An example of complex scene [3].

- *The minimum redundancy of target coverage*

Ensuring the redundancy of observation is mandatory to acquire different perspectives of a target in order to eliminate detection doubts. It consists in the observation of a target by at least two cameras. This is known as *k*-coverage, that is each target has to be observed by at least *k* visual sensor nodes [52]. In our study, we aim to maximize this redundancy, as it can be useful for improving the quality of acquired data and having a fault-tolerant network.

- *The average redundancy ratio*

This metric is inspired by [18]. It indicates the average number of redundant observations over targets. It determines the average number of cameras that can observe each target.

3.3. Communication Metric: The Network Connectivity

In this study, we focus on a distributed network where all cameras perform processing and decision-making, functioning as either relay or sink nodes to enhance fault tolerance. Communication between nodes relies on robust protocols, with direct communication possible only if nodes are within the communication radius (τ_c). Obstacles can weaken signals, reducing effective communication range, and we assume uniform signal attenuation due to obstacles in an indoor environment. To ensure network connectivity, the deployment must guarantee that any pair of nodes is interconnected by some path.

The metrics for connectivity and visual observation, discussed in Sections 3.2 and 3.3, are used as objective functions in our optimization problem. An optimization platform, detailed in Section 4, is employed to address this multi-objective problem.

4. The Proposed Optimization Approach

To address VSN deployment challenges, optimization methods are commonly used to find good solutions. Given the resource and computational demands of exact methods, metaheuristics offer a more efficient alternative. In this study, we utilize a genetic algorithm for optimization, leveraging a platform that integrates both an optimization module and a visual sensor network simulator.

- The optimization module of the platform shown in **Figure 3** enables an efficient exploration of the search space. It generates solutions (composed of the decision variables of the problem) and passes them on to the simulation module for evaluation. We used the well-known NSGA-II [53] genetic algorithm implemented in the jMetal framework [54]. The choice of NSGA-II for this VSN placement problem is justified by its proven ability to efficiently handle multi-objective optimization problems with conflicting criteria, while ensuring good solution diversity.

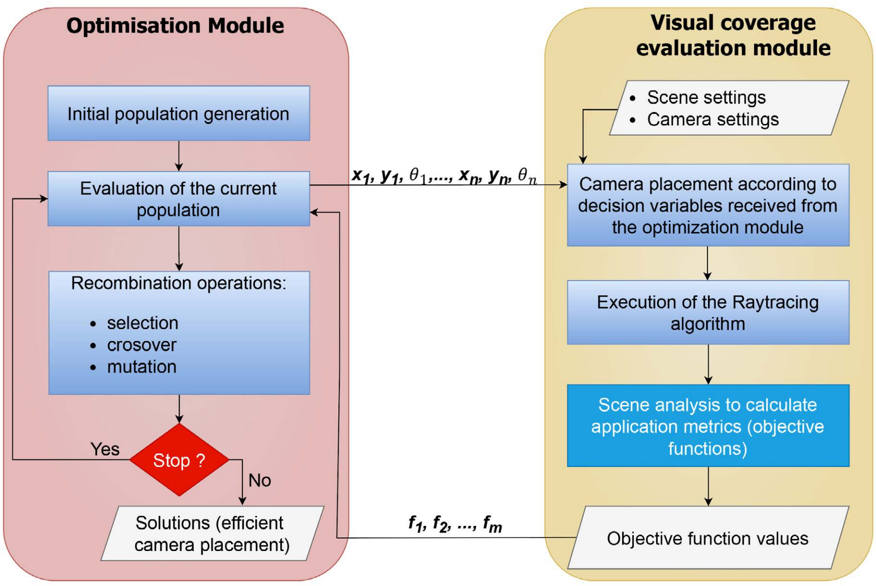

Figure 3. Flowchart of the optimization platform.

- The simulation module on the right describes the study zone (and its parameters) to be evaluated and the deployment of sensors through the decision variables received from the optimization algorithm. This module returns to the optimization module the values of the metrics described in Sections 3.2 and 3.3.

4.1. Annotation Table

Table 1 summarizes some of the annotations used in the paper.

Table 1. Annotations table.

Annotations	Definitions
(x, y)	Camera's position

Continued

θ	Camera's orientation angle
R_c	Communication range
τ_c	Signal attenuation coefficient
$\mathbb{S}$	Set of solutions
$\mathbb{P}$	Set of points
$\mathbb{C}$	Set of cameras
$\mathbb{T}$	Set of targets
$\mathbb{C}_{connex}$	Set of connected components

4.2. Generation of the Initial Population

The optimization process begins with the creation of a randomly generated set of solutions, referred to as the initial population. Each solution consists of the problem's decision variables, which in our case are the cameras' coordinates (x, y) and their orientation angles θ. For a scenario involving n cameras, a solution S is represented as: $S = \{x_1, y_1, \theta_1, x_2, y_2, \theta_2, \cdots, x_n, y_n, \theta_n\}$.

Thus, with n cameras, the problem comprises $3 \times n$ decision variables. Once the initial population is generated, each solution undergoes an evaluation process to assess its quality concerning the problem's objective functions. Specifically, we compute f_1, f_2, f_3, f_4 and f_5 (as defined in Section 4.3). This evaluation is carried out using the simulation module.

4.3. Evaluation of the Population

To assess the solutions, the optimization module sends the decision variables to the simulation module, which evaluates the field of view using the ray-tracing method. To compute the objective function values, the image generated through ray-tracing must be processed. Various techniques exist for extracting relevant information from a rendered scene. One of the most commonly used methods is segmentation [55], an image processing approach that clusters pixels based on shared characteristics, allowing object differentiation. However, not all extracted data are necessarily relevant. To refine the results, the image is further processed by removing noise using mathematical morphology techniques. According to the metrics described in Section 3, five objective functions could be defined as in Sections 3.2 to 3.3.

4.3.1. Overall Coverage Area

Let $\mathbb{P}$ be the set of points on the study field, $\mathbb{C}$ the set of cameras, $\mathbb{T}$ the set of targets and S a deployment solution. The first objective function is the overall coverage area function, f_1, which entails the observation of all pixels in the study field by at least one sensor. Expressed as a percentage, it is calculated using Equation (1).

$$f_1(S)=\frac{\sum_{(x,y)\in\mathbb{P}} obs(x,y)}{|\mathbb{P}|} \tag{1}$$

where $obs(x,y)$ is defined by Equation (2).

$$obs(x,y)=\begin{cases}1 & \text{if } \exists\, c\in\mathbb{C}\,/\,(x,y) \text{ is in FoV of } c\\ 0 & \text{otherwise}\end{cases} \tag{2}$$

4.3.2. Target Coverage

The second objective function, f_2, focuses on target coverage. It involves the observation of targets present in the study field by at least one sensor, calculating the percentage of observed targets (see Equation (3)).

$$f_2(S)=\frac{\sum_{t\in\mathbb{T}} cov(t)}{|\mathbb{T}|} \tag{3}$$

where $cov(t)$ is defined by Equation (4).

$$cov(t)=\begin{cases}1 & \text{if } \exists\, c\in\mathbb{C}\,/\,t \text{ is in the FoV of } c\\ 0 & \text{otherwise}\end{cases} \tag{4}$$

4.3.3. Minimum Redundancy of Target Coverage

The third objective function, denoted as f_3, represents the redundancy in target observation. It involves the observation of targets present in the study field by at least two sensors. The formulation is provided in Equation (5).

$$f_3(S)=\frac{\sum_{t\in\mathbb{T}} Red(t)}{|\mathbb{T}|} \tag{5}$$

where $Red(t)$ is defined by Equation (6).

$$Red(t)=\begin{cases}1 & \text{if } \exists\, c,c'\in\mathbb{C}, c\neq c'\,/\,t \text{ is in } c \text{ and } c'\\ 0 & \text{otherwise}\end{cases} \tag{6}$$

4.3.4. Average Redundancy Ratio

The redundant observation rate, denoted as f_4, quantifies the average number of redundant observations made by the cameras (see Equation (7)).

$$f_4(S)=\frac{\sum_{t\in\mathbb{T}} Views(t)}{|\mathbb{T}|}\times 100 \tag{7}$$

where $Views(t)$ (defined by Equation (8)) returns the number of sensors that can observe $t\in\mathbb{T}$.

$$Views(t)=\begin{cases}n & \text{if } n>1\\ 0 & \text{otherwise}\end{cases} \tag{8}$$

where n is the number of cameras observing t.

4.3.5. Network Connectivity

The fifth objective function (f_5), referred to as connectivity, indicates the number of connected components in the network. It is computed according to Equation (9).

$$f_5(S)=|\mathbb{C}_{connex}| \tag{9}$$

where $\mathbb{C}_{connex}$ represents the set of connected components (see Equation (10)).

A component is said to be connected if and only if, whatever the pair of sensors, there is a path enabling them to communicate.

$$\mathbb{C}_{connex} = \{\mathbb{C}(1), \mathbb{C}(2), \cdots, \mathbb{C}(n)\} \quad (10)$$

where $\mathbb{C}(i)$ is the i^{th} connected component.

Note that given two sensor nodes c and c', they are considered as directly connected if $d(c,c') \le Rc \times \tau_c^q$. Where $d(c,c')$ is the distance between c and c', τ_c is the signal propagation attenuation coefficient and q is the number of obstacles between c and c'.

4.4. Recombination Operators

Following the evaluation phase, solutions are selected for recombination, resulting in the creation of new solutions. This process is inspired by the principles of natural selection. The best solutions will have a better chance of being chosen for recombination and therefore transmission of their characteristics to their offspring. There are several selection operators, such as roulette wheel, selection by rank, selection by tournament, or Boltzmann selection [43] [56]. In our case, solutions are selected for crossover using a roulette wheel operator. The proportion of each solution on the wheel is proportional to its fitness value. This wheel is then rotated at random to select solutions that will help shape the next generation [57]. Each selected pair of solutions, referred to as parents, undergoes recombination through a crossover operator to produce new solutions, known as offspring. The decision variables of the offspring are inherited from the parents. Figure 4 depicts an example of a single-point crossover operation. Various crossover operators exist (single-point crossover, two-point crossover, k-point crossover, uniform crossover, Simulated Binary Crossover, Partially Mapped Crossover, etc). The choice of a crossover operator depends on several criteria, especially the encoding of the decision variables. In our case, we use a single-point crossover since our decision variables are Integer and their number is quite limited. One can observe that decision variables of offspring 1 and offspring 2 are inherited from parents. The mutation step enhances diversity in the optimization process, helping the algorithm escape local optima. For instance, a basic mutation operator can randomly select a decision variable and alter its value.

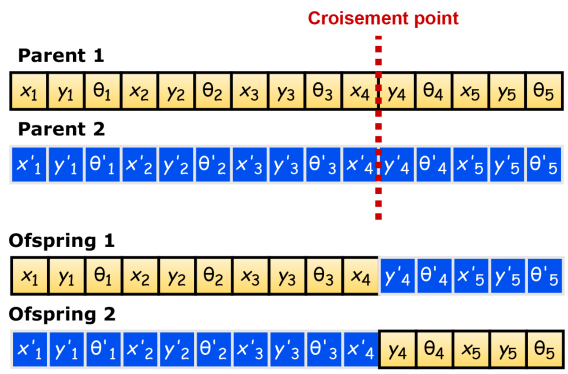

Figure 4. Single-point crossover.

5. Experiments and Results

This paper focuses on the optimization of the deployment of a visual sensor network in an indoor environment. To carry out the simulations, we have implemented a simulation tool based on the ray-tracing method, image segmentation, and filtering. This tool is detailed in Section 4.3. We first consider obstacle-free environments to tackle target coverage issues with respect to redundancy needs. Thereafter, more complex scenarios (with obstacles and communication constraints between sensors) are presented. We evaluate the performances of our method named Optimized Camera Placement Method (OCPM) with respect to some other methods proposed in the literature. This comparison study assesses the adaptability and effectiveness of OCPM.

5.1. Scenes without Obstacle

We compare our method (OCPM) to the approaches presented in [18], while addressing the random deployment of a sensor network for a Redundant Maximization Coverage problem. To strengthen the credibility of this comparative study, we adopted the same simulation parameters as those used in the literature, in which a target is represented by a point.

5.1.1. Simulation Parameters

The visual sensor nodes are randomly deployed. To improve the coverage of targets, the algorithms search for the best orientation angles. Moreover, the algorithms maximize the target observation redundancy. The simulation parameters are presented in **Table 2**. It's important to note that unlike Rangel *et al.*'s work [18], which models a camera's field of view as a triangle, we use a more realistic model (shown in **Figure 1**). In this work, we consider our pixel size to be 4 cm × 4 cm. We consider three objective functions:

Table 2. Simulation parameters.

Study field	500 pixels × 500 pixels
Obstacles	None
Opening angle (α)	60°
Sensing range (R)	70 pixels
Number of sensors	40
Number of targets	50

- *Target coverage*: defined by Equation (3). Each target present in study field is defined by a pixel.
- *Minimum redundancy of target coverage*: defined by Equation (5).
- *Average redundancy ratio*: defined by Equation (7).

Rangel *et al.* [18] use two different approaches to deal with this optimization problem: 1) a lexicographic method where the preferences among the metrics are *a priori* expressed by the decision maker and 2) NSGA-II which is based on Pareto dominance (the preferences among the metrics area *a posteriori* expressed). To make a comparative study possible, we have performed simulations with the same parameters as the NSGA-II method [18].

5.1.2. Results and Comments

Figure 5(a) and **Figure 5(b)** show the minimum and average redundancy results, depending on the target coverage. These results correspond to a set of non-dominated solutions returned by the optimization algorithms: NSGA-II whose performances are taken from [18], OCPM-(θ) where the orientation angles are the only decision variables and OCPM-(x, y, θ) where OCPM has more flexibility (x , y coordinates, as well as the orientation angle θ can be tuned). It is then up to the decision-maker to choose the solution(s) that best correspond(s) to his or her preferences. Each of these solutions is referred to as the best compromise (*Best Compromise*, BC). For NSGA-II, Rangel *et al.* [18] identified the point BC-NSGA-II as the best compromise. For OCPM, the best compromises are respectively marked by the points BC-OCPM (θ) and BC-OCPM (x, y, θ). OCPM-(θ) outperforms NSGA-II (+20% in terms of minimum redundancy and +0.8 for average redundancy). In terms of target observation, OCPM-(θ) reaches 95%. These results can be explained by the effectiveness of our method in ensuring the cameras orientation efficiently, and furthermore the shape of our realistic cone-shaped cameras which improves the evaluation of the cameras' field of view.

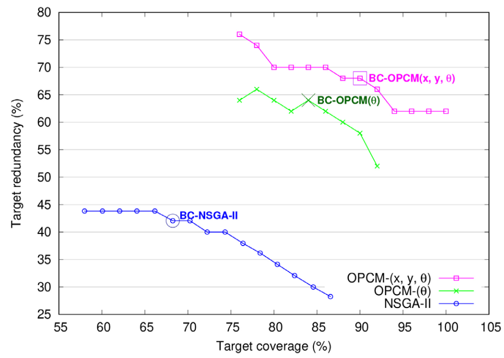

(a)

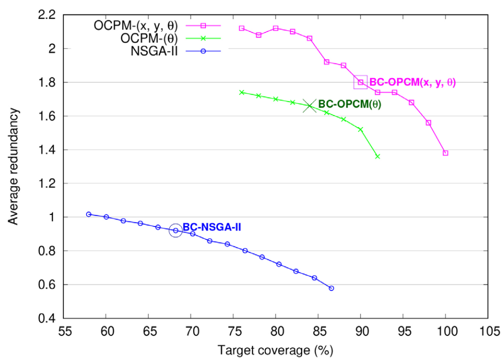

(b)

Figure 5. Comparison of coverage with minimum and average redundancy. (a) Coverage and minimum redundancy results; (b) Coverage and average redundancy results.

OCPM-(x, y, θ) allows the coverage of all the targets (100% of coverage) and its performances are globally better than those of the two other methods. This is explained by the flexibility of the camera positioning and the ability of our method to achieve quickly effective solutions. These preliminary results suggest that our method is more effective than the comparison method in achieving its objectives.

We also compare OCPM to four optimization methods, namely CPGA, ECPGA, Lexicographic and RCMA (these methods and their performances are detailed in [18]). **Figure 6** shows the cumulative values of the best compromise (*Best Compromise*, BC) chosen for each method. We note that OCPM's Best Compromise, in both its versions (BC OCPM-(θ) and BC OCPM-(x, y, θ)), shows higher cumulative objective function values than the other methods. On the other hand, the Lexicographic method outperformed OCPM-(θ) in terms of target coverage. This performance can be explained by the specific optimization process of the lexicographic method, which optimizes each objective function according to a defined order of priority or preference. In this context, the objective optimized first is target coverage, then target redundancy and finally redundancy rate. These initial results show that OCPM is more effective than other methods in the literature in achieving the set objectives.

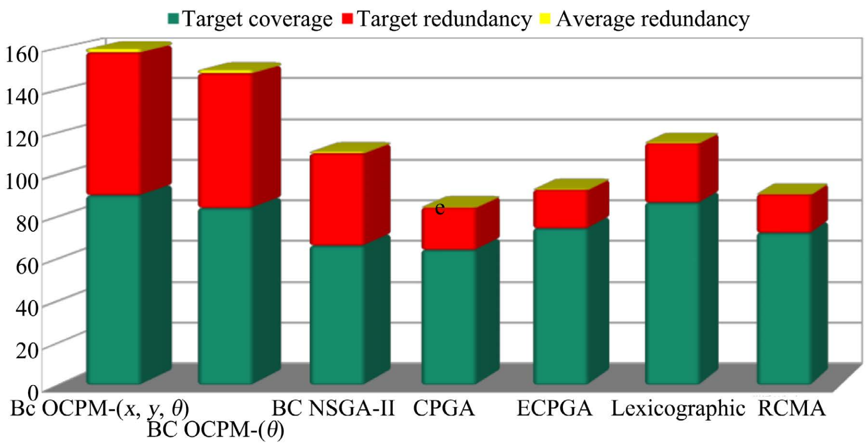

Figure 6. Performance comparison with state-of-art methods.

We carried out further experiments to evaluate the performance of OCPM with respect to the number of visual sensor nodes. For this purpose, we varied the number of cameras from 10 to 70. We considered two scenarios with 25 and 50 randomly placed targets. **Figures 7-9** respectively illustrate the variation in terms of target coverage, minimum redundancy, and average redundancy for a given number of targets and cameras. The presented solutions are selected based on priority, following the order of highest coverage, followed by redundancy, and finally redundancy rate. This selection aligns with the high-speed convergence of our method, adhering to the specified priority order. When the number of cameras is significantly lower than the number of targets, it becomes very difficult to guarantee total coverage. In our case, this situation occurs in the scenario with 10 cameras, where OCPM manages to cover 70% to 75% of the targets.

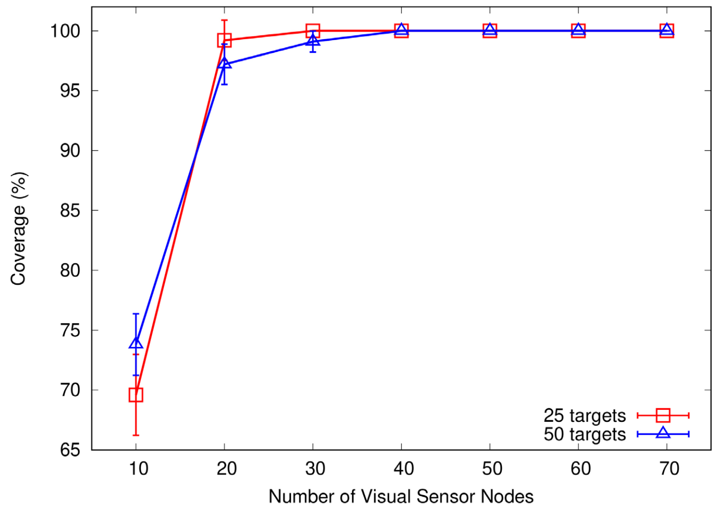

Figure 7. Coverage evolution considering the number of cameras.

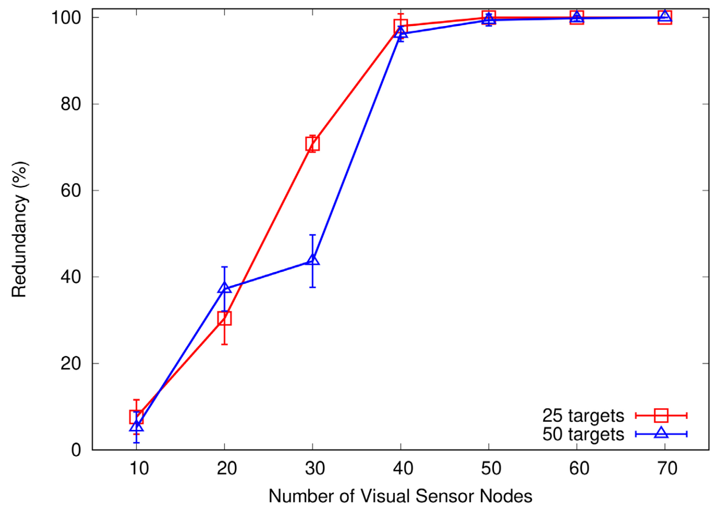

Figure 8. Redundancy evolution considering the number of cameras.

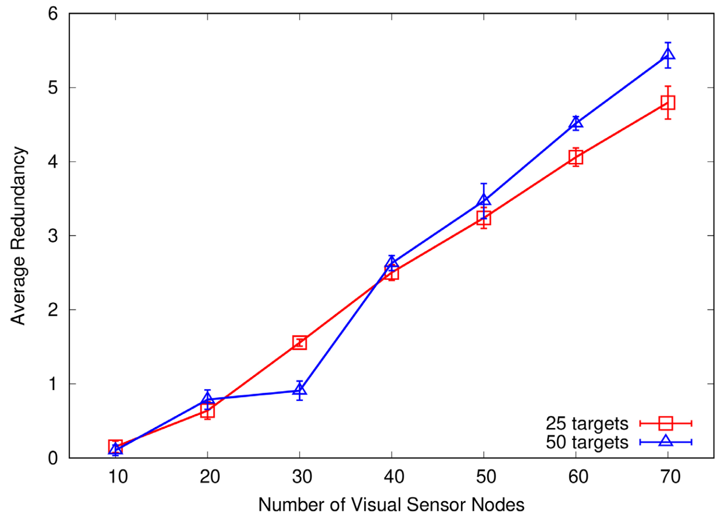

Figure 9. Average redundancy evolution considering the number of cameras.

With a set of 20 cameras, in configurations of 25 and 50 targets, total target coverage is achieved. This improvement in coverage in these configurations helps ensure some redundancy in target observation, ranging between 30% and 40%. The redundancy rate achieved is thus 0.5. These coverage performances are due to a sufficient number of cameras that can cover all targets but are not enough to ensure complete redundant observation of each target.

With a total of 30 cameras, OCPM covers all targets in both configurations. Redundancy becomes easier to ensure, with three-quarters of the 25 targets being redundantly observed. However, in the configuration with 50 targets, OCPM guarantees redundant observation for nearly half of the targets. The average observation rate in both configurations shows that the 25 targets are observed 1.5 times on average redundantly, while the 50 targets are redundantly observed with a rate of 1. This justifies the coverage and redundant observation results. The results for 25 targets can be explained by the Over-provisioned context, where it is easier to meet the objectives, while the configuration with 50 targets represents an Under-provisioned context, where it is harder to reach optimal results with a total of 30 cameras.

With 40 cameras deployed in both configurations, total target coverage is still guaranteed. We then observe maximum redundancy performance for both 25 and 50 targets. Consequently, the average redundancy rate logically increases. In both configurations, the average redundancy rate rises above 2.5, as the first two objectives have nearly reached their maximum values.

With a set of 50 cameras, the results ensure maximum target coverage in configurations with 25 and 50 targets. Redundancy performance is also maximized, due to the significant number of deployed cameras. Thus, the average redundancy rate of the targets is optimized, reaching a value greater than 3, indicating that at least 3 cameras are observing each target. Similarly, tests with 60 and 70 cameras show maximum performance in terms of coverage and redundant observations. In these cases, the redundancy rate will continue to increase as more cameras are added.

These performances allow us to conclude that the proposed robust OCPM approach ensures a certain level of efficiency in solving the optimization problem of VSN deployment. These validations highlight both the Over-provisioned and Under-provisioned contexts, thereby addressing the target coverage problem. It is important to note that in an Under-provisioned context, the standard deviation (error bars) is significant in both configurations. This means the algorithm explores suboptimal solutions, searching a broader space. These error bars indicate the degree of confidence in the results. Since these results represent the best compromise, other solutions may propose higher fitness values for one (or two) objective(s) while degrading the quality of the other(s). As we approach the Over-provisioned context, these error bars decrease or disappear, reinforcing confidence in the optimal values obtained. In this context, OCPM explores a smaller search space, as it meets the application's needs in the Under-provisioned context with a significant number of cameras. Nevertheless, OCPM proves its efficiency and adaptability in solving any type of target coverage problem in both discussed contexts. it's important to note that, unlike [18] which models a camera's field of view as a triangle, we propose a more realistic model of our cameras' fields of view in the form of a circular sector. This increases the size of the cameras' field of view, resulting in a gain. **Figure 10** illustrates this gain in terms of coverage. The gain obtained can be quantified by calculating the difference between the area of the circular sector and the area of the triangle (see Equation (11)).

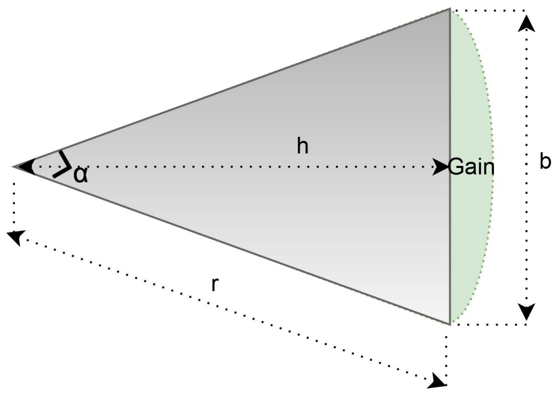

Figure 10. Graphical representation of visual coverage gain.

$$Gain = \frac{\alpha \pi r^2}{360} - \frac{b \times h}{2} = \frac{\frac{\alpha \pi}{360} - \gamma\sqrt{1-\gamma^2}}{\gamma\sqrt{1-\gamma^2}} \tag{11}$$

where $\gamma = \sin\left(\frac{\alpha}{2}\right)$.

Otherwise, we systematically varied the number of cameras and targets, yielding compelling solutions. Furthermore, the challenge intensifies when acquiring scene data in the presence of physical obstacles. In the subsequent section, we enhance our approach by incorporating these features in the analysis of a complex scene with obstructions.

5.2. Scene with Obstacles

In the following, we have made the scene more complex by integrating obstacles and zones of interest. This poses a significant challenge in this field, as the objective is to maximize various functions that may be impeded by the presence of obstacles.

- *Overall coverage* (denoted f_1): is defined in Equation (1).
- *Target coverage* (denoted f_2): it is defined in Equation (3).
- *Redundant target coverage* (denoted f_3): it is defined in Equation (5).

We address the presence of obstructions without delving into the specific nature of the objects causing the obstructions. We consider obstacles that obstruct the field of view of the cameras, as shown in **Figure 11** with sizes 1400 × 700. We place cameras on walls for possible support or power supply. Each camera has an observation range of 700 pixels. This scene consists of 5 cameras. Additionally, there are 6 zones of interest, resembling a building structure. The description of walls and zones of interest can be found in Section 3.2.

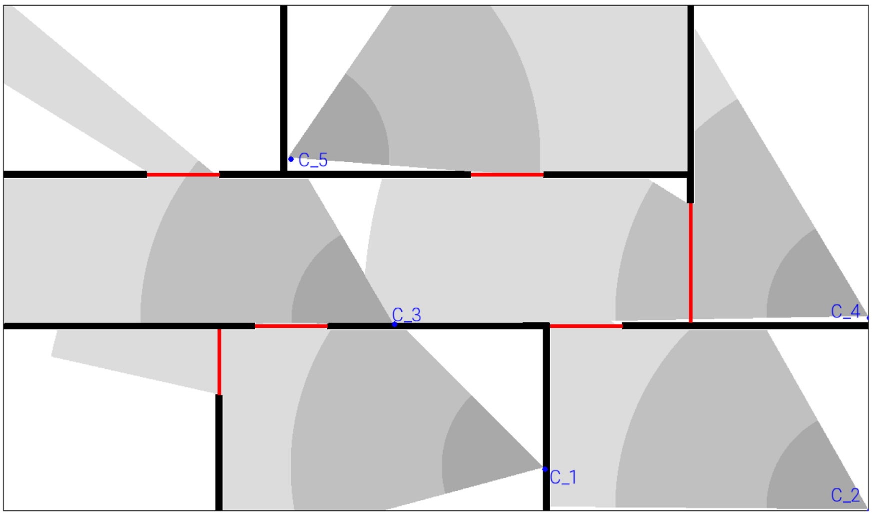

Figure 11. Scene with 5 cameras considering obstacles.

To extend our tests, we consider scenarios with 5, 12 and 20 cameras. This allows us to deal with underprovisioned and over provisioned applications. We consider a zone of interest as covered if at least 80% of its area is observed by cameras. The redundancy optimized here is the smallest value of all the zones of interest. If a redundancy of 100% of targets is noted, then all targets are redundantly observed. If zero redundancy is noted, this means that there is at least one zone of interest that is not observed redundantly.

Figure 12 shows the diagrams illustrating the cumulative objective values of the solutions obtained for each deployment. The presence of obstacles in a scene introduces complexity to the acquisition of scene information. We observe that, with 5 cameras in the under-provisioned context, our method allows an overall coverage ranging from 58% to 66%. This could be attributed to the limitations in the field of view and the constrained number of cameras deployed. The algorithm then seeks to guarantee coverage of the zones of interest between 83% and 100%, but without guaranteeing the total redundancy of target zones in account of the insufficient number of cameras. In the over provisioned context, with twice as many cameras as zones of interest, the overall coverage achieved is 92%, with target zone coverage ranging from 98.5% to 100%. Target redundancy therefore reaches 100%, meaning that we can observe redundantly all the targets. These values can be explained by a sufficient number of cameras in the study zone. With 20 cameras, the algorithm proposes an overall coverage of between 96% and 98% for a target zone coverage of 100%. The smallest redundancy recorded is 30%. However, in most cases it reaches 100%.

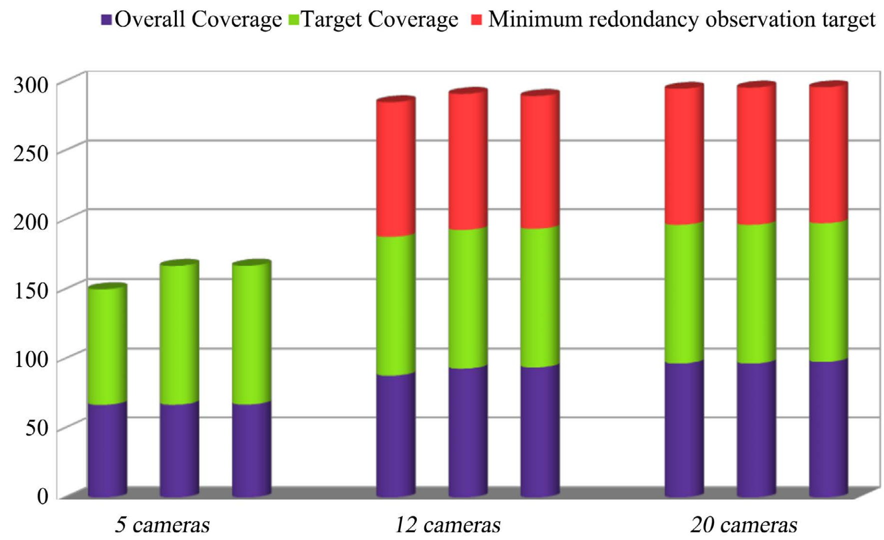

Figure 12. Deployment of 5 - 12 - 20 cameras considering 6 zones of interest.

In an under provisioned context, achieving maximum objective values is more complicated when obstacles are present. This can be explained by an insufficient number of sensors and complexity of scene. However, targets are observed at 100%. The algorithm converges to achieve 100% for all objective functions with twice as many cameras as targets. Cumulative solutions' score is close to 280. Note that our method succeeds in proposing better solutions for target observation at 100% in different tests, which is essential and principal measurement are monitored in several applications in VSN.

5.3. Considering Communication Requirement and Constraints

To ensure global communication within the network, the nodes should be connected and able to transmit data. This data transfer occurs either directly from a sensor node to the sink node (single-hop communication) or through neighboring nodes, ultimately reaching the sink node (multi-hop communication) [42]. Depending on the application, it is possible to define several connected components to streamline resource usage. Optimizing the number of connected components in the network is a non-trivial task. This optimization process entails minimizing the number of connected components (the optimum being to have a single connected component). In this paper, we consider communications that use omnidirectional wireless within an environment with obstacles (both with visual and communication obstacles). When crossing an obstacle, the communication radius (Rc) between nodes decreases according to the signal propagation attenuation coefficient τ. This means that given two sensor nodes c and c' they can directly communicate (a point-to-point communication) if $d(c,c') \le Rc \times \tau_c^q$. Where q is the number of obstacle between c and c'. For our experiments, we consider $\tau = 50\%$. Note that the communication radius considered here is equal to the camera range. The best solutions are chosen based on priority, with connectivity being the primary consideration in this network type. It is followed by the redundancy observation of targets present in the scene and, finally, the goal of achieving overall coverage. The objective is to:

- Ensure a connected network with one related component (f_5): expressed in Equation (9).
- Observe all targets (f_2 and f_3): illustrated in Equations (3) and (5).
- Maximize the coverage of the entire study zone (f_1): shown in Equation (1).

Figure 13(a) and Figure 14(a) showcase the deployment results of our cameras to ensure overall and target coverage. In Figure 13(b) and Figure 14(b), all existing links between nodes are represented by the green line, organized in batches. Figure 13(a) illustrates the result of scene implemented in the previous section for 12 cameras, integrating communication on the nodes.

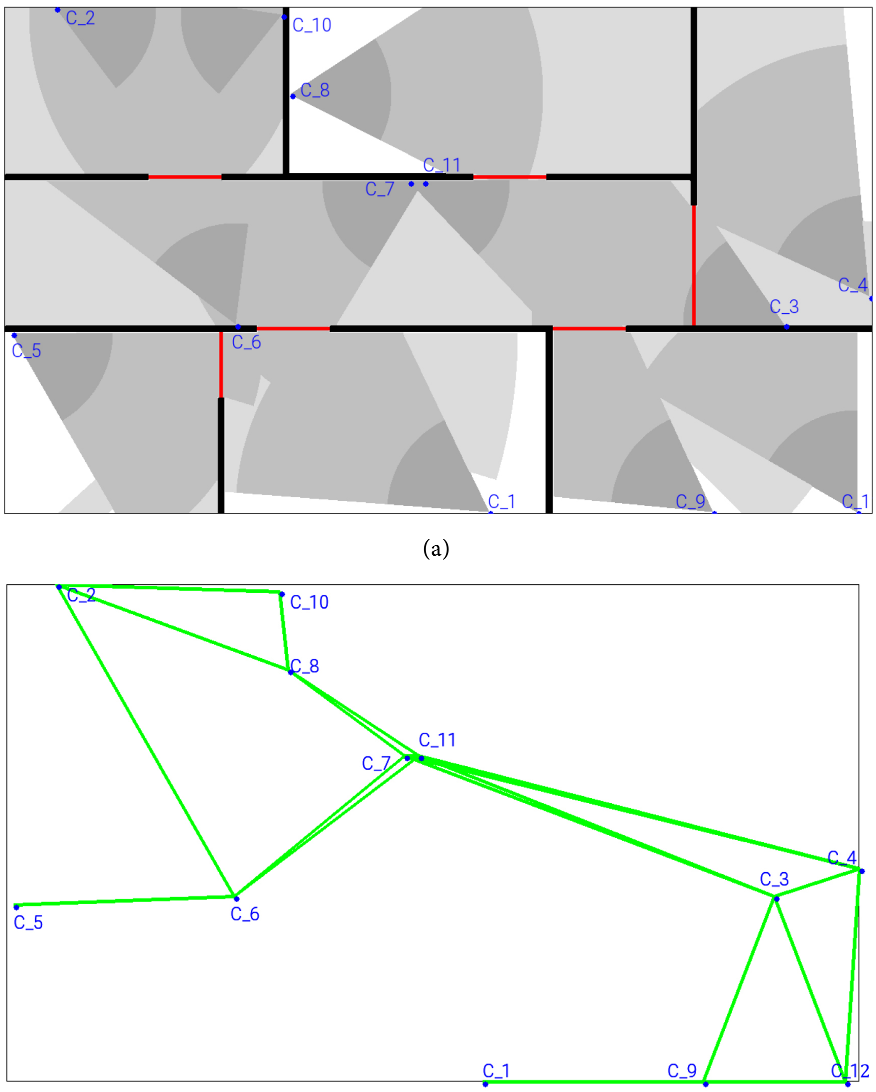

(a)

(b)

Figure 13. Deployment and connectivity of 12 cameras in the indoor scene. (a) Deployment of 12 cameras in an indoor scene, (b) Resulting connectivity with 12 cameras.

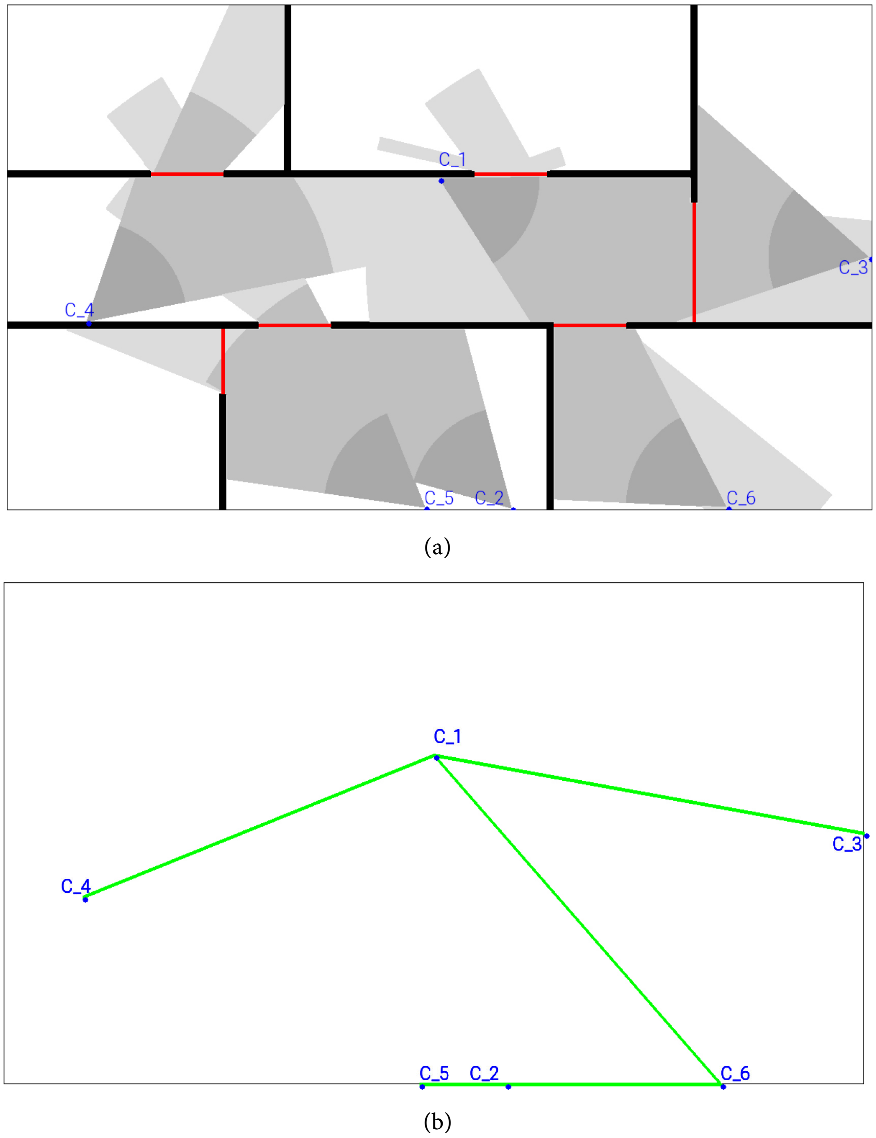

Figure 14. Deployment and connectivity of 6 cameras in the indoor scene. (a) Deployment of 6 cameras in an indoor scene, (b) Resulting connectivity with 6 cameras.

The overall coverage of the scene varies between 82% and 98%, justified by the excess over-provisioned deployment, while that of the target zones reaches 100%. With a doubled number of cameras, our method returns solutions that strike a compromise between coverage and target redundancy. Importantly, our method successfully proposes a better compromise with a redundancy value of almost 98%. At this point, the number of related components of the network is equal to 1, as seen in Figure 13(b). Note that cameras C_7 and C_{11} are not directly connected to C_{10} due to obstruction by two obstacles which attenuate the communication range. However, a multi-hop link is available for them. Therefore, we run simulations with a number of cameras equal to that of the targets, as in Figure 14(a). The best selected compromise yielded a connectivity result of 1, as shown in Figure 14(b).

The algorithm positioned the cameras to cover all targets at 100% and redundantly at 90%. The performance of overall coverage achieves 63%, attributed to the observation limit of the cameras. Cameras C_3 and C_6 are not evenly connected due to the presence of an obstacle between the two cameras which degrades the communication range. These results illustrate the effectiveness and adaptability of our approach. Moreover, the literature rarely tackles multi-objective optimization of all these criteria simultaneously. This allows us to emphasize the contributions of our method.

6. Conclusion

This paper focuses on the effective placement of visual sensor nodes in indoor environments and introduces a multi-objective optimization technique named OCPM. The method shows great potential for applications in computer vision, visual detection, and target tracking. Scalable approaches have proven to be robust in exploring a broad solution space, resulting in an optimal camera placement that surpasses traditional methods. Initially, the focus was on optimizing target coverage and redundancy in a simplified context. Subsequently, free camera placement was allowed, ensuring both target coverage and redundancy. A comparative study shows that OCPM provides better solutions, demonstrating its adaptability and the efficiency of genetic algorithms in optimizing the performance of visual sensor networks. Cameras were placed considering obstacles, target areas, and connectivity between sensors. The results cover all targets while maintaining network connectivity for data transfer. In both over- and under-provisioned contexts, the method achieves maximum coverage or at least 50% of the scene. This approach benefits fields like object detection, image segmentation, and building monitoring. Achieving these results (e.g., 98% redundancy) ensures continuous monitoring of targets, even in the presence of occlusions or sensor failures, thereby directly enhancing the reliability of applications such as intruder tracking and activity recognition. This highlights the practical applicability of the proposed OCPM method for real-world deployment of visual sensor networks. Future challenges include addressing device failure, reducing power consumption, and integrating mobile cameras for improved reliability.

7. Limitations

Despite its promising results, this study is subject to several limitations that may affect real-world deployment. First, the environment is modeled in 2D, neglecting vertical complexity, which may influence coverage and connectivity in multi-level or cluttered indoor spaces. Second, cameras are assumed fixed, without tilt or zoom, limiting flexibility compared to actual systems that can adjust dynamically. Third, the signal propagation model uses uniform attenuation coefficients for obstacles, whereas real materials may cause variable losses. Additionally, the current approach does not account for device failures, energy constraints, or mobile cameras, which are critical factors in practical visual sensor networks. While these simplifications facilitate optimization and comparative studies, they highlight areas for future work to ensure reliable and efficient deployment in complex indoor environments.

Conflicts of Interest

The authors declare no conflicts of interest regarding the publication of this paper.

References

[1] Soro, S. and Heinzelman, W. (2009) A Survey of Visual Sensor Networks. *Advances in Multimedia*, **2009**, 1-21. https://doi.org/10.1155/2009/640386

[2] Chakrabarty, K., Iyengar, S.S., Qi, H.R. and Cho, E. (2002) Grid Coverage for Surveillance and Target Location in Distributed Sensor Networks. *IEEE Transactions on Computers*, **51**, 1448-1453. https://doi.org/10.1109/tc.2002.1146711

[3] Marroquin, R., Dubois, J. and Nicolle, C. (2019) Wisenet: An Indoor Multi-Camera Multi-Space Dataset with Contextual Information and Annotations for People Detection and Tracking. *Data in Brief*, **27**, Article 104654. https://doi.org/10.1016/j.dib.2019.104654

[4] Ojha, T., Misra, S. and Raghuwanshi, N.S. (2015) Wireless Sensor Networks for Agriculture: The State-of-the-Art in Practice and Future Challenges. *Computers and Electronics in Agriculture*, **118**, 66-84. https://doi.org/10.1016/j.compag.2015.08.011

[5] Durisic, M.P., Tafa, Z., Dimic, G. and Milutinovic, V. (2012) A Survey of Military Applications of Wireless Sensor Networks. 2012 *Mediterranean Conference on Embedded Computing* (*MECO*), Bar, 19-21 June 2012, 196-199.

[6] Faga, Y., Abdou, W. and Dubois, J. (2023) An Optimised Indoor Deployment of Visual Sensor Networks. *IEEE SITIS Conference*, Bangkok, 8-10 November 2023, 1-8.

[7] Charfi, Y., Wakamiya, N. and Murata, M. (2009) Challenging Issues in Visual Sensor Networks. *IEEE Wireless Communications*, **16**, 44-49. https://doi.org/10.1109/mwc.2009.4907559

[8] Njoya, A.N., Ari, A.A.A., Nana Awa, M., Titouna, C., Labraoui, N., Effa, J.Y., *et al.* (2020) Hybrid Wireless Sensors Deployment Scheme with Connectivity and Coverage Maintaining in Wireless Sensor Networks. *Wireless Personal Communications*, **112**, 1893-1917. https://doi.org/10.1007/s11277-020-07132-5

[9] Senouci, M.R., Mellouk, A. and Aissani, A. (2014) Random Deployment of Wireless Sensor Networks: A Survey and Approach. *International Journal of Ad Hoc and Ubiquitous Computing*, **15**, 133-146. https://doi.org/10.1504/ijahuc.2014.059905

[10] Abdulwahid, H.M. and Mishra, A. (2022) Deployment Optimization Algorithms in Wireless Sensor Networks for Smart Cities: A Systematic Mapping Study. *Sensors*, **22**, Article 5094. https://doi.org/10.3390/s22145094

[11] Costa, D.G. and Guedes, L.A. (2010) The Coverage Problem in Video-Based Wireless Sensor Networks: A Survey. *Sensors*, **10**, 8215-8247. https://doi.org/10.3390/s100908215

[12] Evangelakos, E.A., Kandris, D., Rountos, D., Tselikis, G. and Anastasiadis, E. (2022) Energy Sustainability in Wireless Sensor Networks: An Analytical Survey. *Journal of Low Power Electronics and Applications*, **12**, Article 65. https://doi.org/10.3390/jlpea12040065

[13] Wang, Z.H. and Wang, F. (2019) Wireless Visual Sensor Networks: Applications, Challenges, and Recent Advances. 2019 *SoutheastCon*, Huntsville, 11-14 April 2019,

1-8. https://doi.org/10.1109/southeastcon42311.2019.9020600

[14] Pan, L.G. (2020) Preventing Forest Fires Using a Wireless Sensor Network. *Journal of Forest Science*, **66**, 97-104. https://doi.org/10.17221/151/2019-jfs

[15] Hsu, Y.C., Chen, Y.T. and Liang, C.K. (2011) The Coverage Problem in Directional Sensor Networks with Rotatable Sensors. In: *Lecture Notes in Computer Science*, Springer, 450-462. https://doi.org/10.1007/978-3-642-23641-9_36

[16] Mnasri, S., Thaljaoui, A., Nasri, N. and Val, T. (2015) A Genetic Algorithm-Based Approach to Optimize the Coverage and the Localization in the Wireless Audio-Sensors Networks. 2015 *International Symposium on Networks, Computers and Communications* (*ISNCC*), Yasmine Hammamet, 13-15 May 2015, 1-6. https://doi.org/10.1109/isncc.2015.7238591

[17] Fu, J.Y., Li, X.L., Li, Y.L. and Dong, X. (2022) Coverage Control for Directional Sensor Networks with Visual Sensing Constraints. 2022 *IEEE International Conference on Unmanned Systems* (*ICUS*), Guangzhou, 28-30 October 2022, 387-392. https://doi.org/10.1109/icus55513.2022.9986941

[18] Rangel, E.O., Costa, D.G. and Loula, A. (2019) On Redundant Coverage Maximization in Wireless Visual Sensor Networks: Evolutionary Algorithms for Multi-Objective Optimization. *Applied Soft Computing*, **82**, Article 105578. https://doi.org/10.1016/j.asoc.2019.105578

[19] Cheng, C.F. and Tsai, K.T. (2015) Barrier Coverage in Wireless Visual Sensor Networks with Importance of Image Consideration. 2015 *Seventh International Conference on Ubiquitous and Future Networks*, Sapporo, 7-10 July 2015, 793-798. https://doi.org/10.1109/icufn.2015.7182651

[20] Ai, J. and Abouzeid, A.A. (2006) Coverage by Directional Sensors in Randomly Deployed Wireless Sensor Networks. *Journal of Combinatorial Optimization*, **11**, 21-41. https://doi.org/10.1007/s10878-006-5975-x

[21] Osais, Y.E., St-Hilaire, M. and Yu, F.R. (2008) Directional Sensor Placement with Optimal Sensing Range, Field of View and Orientation. *Mobile Networks and Applications*, **15**, 216-225. https://doi.org/10.1007/s11036-009-0179-0

[22] Katti, A. and Lobiyal, D.K. (2017) Node Deployment Strategies for a 2D Wireless Sensor Network. *2017 International Conference on Computing, Communication and Automation* (*ICCCA*), Greater Noid, 5-6 May 2017, 658-663. https://doi.org/10.1109/ccaa.2017.8229883

[23] Hajizadeh, N., Javidan, R., Shamsinejad, P. and Akbari, R. (2020) Node Deployment in Wireless Sensor Networks Using the New Multi-Objective Levy Flight Bee Algorithm. *IET Wireless Sensor Systems*, **10**, 78-87. https://doi.org/10.1049/iet-wss.2019.0083

[24] Choudhary, M. and Goyal, N. (2021) Node Deployment Strategies in Underwater Wireless Sensor Network. 2021 *International Conference on Advance Computing and Innovative Technologies in Engineering* (*ICACITE*), Greater Noida, 4-5 March 2021, 773-779. https://doi.org/10.1109/icacite51222.2021.9404617

[25] Osamy, W., Khedr, A.M., Salim, A., Ali, A.I.A. and El-Sawy, A.A. (2022) Coverage, Deployment and Localization Challenges in Wireless Sensor Networks Based on Artificial Intelligence Techniques: A Review. *IEEE Access*, **10**, 30232-30257. https://doi.org/10.1109/access.2022.3156729

[26] Priyadarshi, R., Gupta, B. and Anurag, A. (2020) Deployment Techniques in Wireless Sensor Networks: A Survey, Classification, Challenges, and Future Research Issues. *The Journal of Supercomputing*, **76**, 7333-7373. https://doi.org/10.1007/s11227-020-03166-5

[27] Cao, L., Yue, Y.G., Cai, Y. and Zhang, Y. (2021) A Novel Coverage Optimization Strategy for Heterogeneous Wireless Sensor Networks Based on Connectivity and Reliability. *IEEE Access*, **9**, 18424-18442. https://doi.org/10.1109/access.2021.3053594

[28] Afghantoloee, A. and Mostafavi, M.A. (2021) A Local 3D Voronoi-Based Optimization Method for Sensor Network Deployment in Complex Indoor Environments. *Sensors*, **21**, Article 8011. https://doi.org/10.3390/s21238011

[29] Nasri, N., Mnasri, S. and Val, T. (2020) 3D Node Deployment Strategies Prediction in Wireless Sensors Network. *International Journal of Electronics*, **107**, 808-838. https://doi.org/10.1080/00207217.2019.1687759

[30] Vidhya, J., Prasanna, P., Margarat, M. and Jayalakshmy, S. (2021) Enhancing Network Coverage Using Sensing Models in Wireless Sensor Network. *Journal of Physics: Conference Series*, **1717**, Article 012062. https://doi.org/10.1088/1742-6596/1717/1/012062

[31] Saad, A., Senouci, M.R. and Benyattou, O. (2020) Toward a Realistic Approach for the Deployment of 3D Wireless Sensor Networks. *IEEE Transactions on Mobile Computing*, **21**, 1508-1519. https://doi.org/10.1109/tmc.2020.3024939

[32] Jesus, T.C., Costa, D.G., Portugal, P. and Vasques, F. (2022) A Survey on Monitoring Quality Assessment for Wireless Visual Sensor Networks. *Future Internet*, **14**, Article 213. https://doi.org/10.3390/fi14070213

[33] Costa, D.G., Silva, I., Guedes, L.A., Portugal, P. and Vasques, F. (2014) Selecting Redundant Nodes When Addressing Availability in Wireless Visual Sensor Networks. 2014 12*th IEEE International Conference on Industrial Informatics* (*INDIN*), Porto Alegre, 27-30 July 2014, 130-135. https://doi.org/10.1109/indin.2014.6945496

[34] Costa, D.G., Vasques, F. and Portugal, P. (2017) Enhancing the Availability of Wireless Visual Sensor Networks: Selecting Redundant Nodes in Networks with Occlusion. *Applied Mathematical Modelling*, **42**, 223-243. https://doi.org/10.1016/j.apm.2016.10.008

[35] Alaei, M. and Barcelo-Ordinas, J.M. (2010) Node Clustering Based on Overlapping Fovs for Wireless Multimedia Sensor Networks. 2010 *IEEE Wireless Communication and Networking Conference*, Sydney, 18-21 April 2010, 1-6. https://doi.org/10.1109/wcnc.2010.5506615

[36] Rangel, E.O., Costa, D.G. and Loula, A. (2018) Redundant Visual Coverage of Prioritized Targets in IoT Applications. *Proceedings of the* 24*th Brazilian Symposium on Multimedia and the Web*, Salvador, 16-19 October 2018, 307-314. https://doi.org/10.1145/3243082.3243090

[37] Hefeeda, M. and Bagheri, M. (2007) Randomized K-Coverage Algorithms for Dense Sensor Networks. *IEEE INFOCOM* 2007 26*th IEEE International Conference on Computer Communications*, Anchorage, 6-12 May 2007, 2376-2380. https://doi.org/10.1109/infcom.2007.284

[38] Malek, S.M.B., Sadik, M.M. and Rahman, A. (2016) On Balanced K-Coverage in Visual Sensor Networks. *Journal of Network and Computer Applications*, **72**, 72-86. https://doi.org/10.1016/j.jnca.2016.06.011

[39] Altahir, A.A., Asirvadam, V.S., Hamid, N.H.B., Sebastian, P., Saad, N.B., Ibrahim, R.B., *et al.* (2018) Optimizing Visual Sensor Coverage Overlaps for Multiview Surveillance Systems. *IEEE Sensors Journal*, **18**, 4544-4552. https://doi.org/10.1109/jsen.2018.2825781

[40] Costa, D.G., Silva, I., Guedes, L.A., Vasques, F. and Portugal, P. (2015) Optimal Sensing Redundancy for Multiple Perspectives of Targets in Wireless Visual Sensor Net-

works. 2015 *IEEE 13th International Conference on Industrial Informatics* (*INDIN*), Cambridge, 22-24 July 2015, 185-190. https://doi.org/10.1109/indin.2015.7281732

[41] Costa, D.G., Silva, I., Guedes, L.A., Portugal, P. and Vasques, F. (2014). Enhancing Redundancy in Wireless Visual Sensor Networks for Target Coverage. *Proceedings of the 20th Brazilian Symposium on Multimedia and the Web*, João Pessoa, 18-21 November , 31-38. https://doi.org/10.1145/2664551.2664558

[42] Farsi, M., Elhosseini, M.A., Badawy, M., Arafat Ali, H. and Zain Eldin, H. (2019) Deployment Techniques in Wireless Sensor Networks, Coverage and Connectivity: A Survey. *IEEE Access*, **7**, 28940-28954. https://doi.org/10.1109/access.2019.2902072

[43] Tossa, F., Abdou, W., Ansari, K., Ezin, E.C. and Gouton, P. (2022) Area Coverage Maximization under Connectivity Constraint in Wireless Sensor Networks. *Sensors*, **22**, Article 1712. https://doi.org/10.3390/s22051712

[44] Ahn, J.W., Chang, T.W., Lee, S.H. and Seo, Y. (2016) Two-Phase Algorithm for Optimal Camera Placement. *Scientific Programming*, **2016**, 1-16. https://doi.org/10.1155/2016/4801784

[45] Bouzid, S.E., Seresstou, Y., Raoof, K., Omri, M.N., Mbarki, M. and Dridi, C. (2020) MOONGA: Multi-Objective Optimization of Wireless Network Approach Based on Genetic Algorithm. *IEEE Access*, **8**, 105793-105814. https://doi.org/10.1109/access.2020.2999157

[46] Kavitha Rani, P., Chae, H., Nam, Y. and Abouhawwash, M. (2023) Energy-Efficient Clustering Using Optimization with Locust Game Theory. *Intelligent Automation & Soft Computing*, **36**, 2591-2605. https://doi.org/10.32604/iasc.2023.033697

[47] Ajmi, N., Helali, A., Lorenz, P. and Mghaieth, R. (2021) Mwcsga-Multi Weight Chicken Swarm Based Genetic Algorithm for Energy Efficient Clustered Wireless Sensor Network. *Sensors*, **21**, Article 791. https://doi.org/10.3390/s21030791

[48] Silva, T.F. and Costa, D.G. (2016) Centralized Algorithms for Redundant Coverage Maximization in Wireless Visual Sensor Networks. *IEEE Latin America Transactions*, **14**, 3378-3384. https://doi.org/10.1109/tla.2016.7587645

[49] Halé, A., Trouvé-Peloux, P. and Volatier, J.-B. (2021) End-to-End Sensor and Neural Network Design Using Differential Ray Tracing. *Optics Express*, **29**, Article 34748. https://doi.org/10.1364/oe.439571

[50] Alwajeeh, T., Combeau, P. and Aveneau, L. (2020) An Efficient Ray-Tracing Based Model Dedicated to Wireless Sensor Network Simulators for Smart Cities Environments. *IEEE Access*, **8**, 206528-206547. https://doi.org/10.1109/access.2020.3037135

[51] Gómez, J., Tayebi, A., Hellín, C.J., Valledor, A., Barranquero, M. and Cuadrado-Gallego, J.J. (2023) Accelerated Ray Launching Method for Efficient Field Coverage Studies in Wide Urban Areas. *Sensors*, **23**, Article 6412. https://doi.org/10.3390/s23146412

[52] Mini, S., Udgata, S.K. and Sabat, S.L. (2014) Sensor Deployment and Scheduling for Target Coverage Problem in Wireless Sensor Networks. *IEEE Sensors Journal*, **14**, 636-644. https://doi.org/10.1109/jsen.2013.2286332

[53] Deb, K., Pratap, A., Agarwal, S. and Meyarivan, T. (2002) A Fast and Elitist Multi-Objective Genetic Algorithm: Nsga-II. *IEEE Transactions on Evolutionary Computation*, **6**, 182-197. https://doi.org/10.1109/4235.996017

[54] Durillo, J.J. and Nebro, A.J. (2011) jMetal: A Java Framework for Multi-Objective Optimization. *Advances in Engineering Software*, **42**, 760-771. https://doi.org/10.1016/j.advengsoft.2011.05.014

[55] Gao, K., Wang, H. and Nazarko, J. (2022) An Efficient Data Acquisition and Pro-

cessing Scheme for Wireless Multimedia Sensor Networks. *Computational Intelligence and Neuroscience*, **2022**, 1-14. https://doi.org/10.1155/2022/6394029

[56] Gupta, S.K., Kuila, P. and Jana, P.K. (2016) Genetic Algorithm Approach for K-Coverage and M-Connected Node Placement in Target Based Wireless Sensor Networks. *Computers & Electrical Engineering*, **56**, 544-556. https://doi.org/10.1016/j.compeleceng.2015.11.009

[57] Katoch, S., Chauhan, S.S. and Kumar, V. (2020) A Review on Genetic Algorithm: Past, Present, and Future. *Multimedia Tools and Applications*, **80**, 8091-8126. https://doi.org/10.1007/s11042-020-10139-6